European Journal of Immunology

Alterations to chromatin in intestinal macrophages link IL-10 deficiency to inappropriate inflammatory responses

Jeremy M. Simon[1], James P. Davis[1], Saangyoung E. Lee[1], Matthew R. Schaner[1], Gregory R. Gipson[1], Matthew Weiser[1,2], R. Balfour Sartor[3,4,5], Hans H. Herfarth[3,4], Reza Rahbar[6], Timothy S. Sadiq[6], Mark J. Koruda[6], Dermot P. McGovern[7], Jason D. Lieb[8], Karen L. Mohlke[1], Terrence S. Furey[1,9] and Shehzad Z. Sheikh*[1,3,4]*

[1] Department of Genetics, University of North Carolina, Chapel Hill, NC, USA
[2] Curriculum in Bioinformatics and Computational Biology, University of North Carolina, Chapel Hill, NC, USA
[3] Center for Gastrointestinal Biology and Disease, University of North Carolina, Chapel Hill, NC, USA
[4] Department of Medicine, Division of Gastroenterology and Hepatology, University of North Carolina, Chapel Hill, NC, USA
[5] Department of Microbiology and Immunology, University of North Carolina, Chapel Hill, NC, USA
[6] Department of Surgery, University of North Carolina, Chapel Hill, NC, USA
[7] F. Widjaja Foundation Inflammatory Bowel and Immunobiology Research Institute, Cedars-Sinai Medical Center, Los Angeles, CA, USA
[8] Department of Human Genetics, University of Chicago, IL, USA
[9] Department of Biology, University of North Carolina, Chapel Hill, NC, USA

Intestinal macrophages (IMs) are uniquely programmed to tolerate exposure to bacteria without mounting potent inflammatory responses. The cytokine IL-10 maintains the macrophage anti-inflammatory response such that loss of IL-10 results in chronic intestinal inflammation. To investigate how IL-10-deficiency alters IM programming and bacterial tolerance, we studied changes in chromatin accessibility in response to bacteria in macrophages from two distinct niches, the intestine and bone-marrow, from both wild-type and IL-10-deficient (*Il10*$^{-/-}$) mice. We identified chromatin accessibility changes associated with bacterial exposure and IL-10 deficiency in both bone marrow derived macrophages and IMs. Surprisingly, *Il10*$^{-/-}$ IMs adopted chromatin and gene expression patterns characteristic of an inflammatory response, even in the absence of bacteria. Further, when recombinant IL-10 was added to *Il10*$^{-/-}$ cells, it could not revert the chromatin landscape to a normal state. Our results demonstrate that IL-10 deficiency results in stable chromatin alterations in macrophages, even in the absence of bacteria. This supports a model in which IL-10-deficiency leads to chromatin alterations that contribute to a loss of IM tolerance to bacteria, which is a primary initiating event in chronic intestinal inflammation.

Keywords: Chromatin accessibility · Chronic inflammation · IL-10 · Inflammatory bowel disease · Macrophages

Additional supporting information may be found in the online version of this article at the publisher's web-site

Correspondence: Dr. Shehzad Z. Sheikh
e-mail: sheisx@med.unc.edu

*These authors contributed equally to this work.

Introduction

Crohn's disease (CD) is a chronic intestinal inflammatory disorder driven by a combination of genetic and environmental factors, the intestinal bacteria, and the immune system [1]. The lamina propria tissue layer in the intestine is composed of multiple immune cell types, including macrophages, B cells, and T cells, which are separated from the intestinal bacteria by a single layer of epithelial cells. Intestinal macrophages (IMs) have adapted a unique tolerance to the intestinal environment by effectively killing bacteria that breach this epithelial barrier through phagocytosis, but unlike macrophages from other tissues, do not mount a cytokine-mediated inflammatory response thereby preventing damage to surrounding tissue [2]. These mechanisms fail during CD pathogenesis [3]. In contrast, bacteria-induced changes to histone modifications, transcription factor binding, and transcription reflective of vigorous inflammation have been characterized in bone marrow derived macrophages (BMMs) [4–6].

IL-10 maintains the IM anti-inflammatory response, and its expression increases when these cells are exposed to bacteria [7, 8]. Intestinal inflammation is not observed when IL-10-deficient (*Il10*$^{-/-}$) mice are raised in a germ-free (GF) environment lacking bacteria, but emerges when mice are conventionally raised (CR) with bacteria present or after colonization of GF *Il10*$^{-/-}$ mice with normal intestinal bacteria [9]. More specifically, compared to macrophages from wild-type (WT) mice, inflammatory responses to bacterial stimuli are more vigorous in *Il10*$^{-/-}$ bone marrow derived macrophages (BMMs) and aberrantly arise in *Il10*$^{-/-}$ IMs [10–12].

In this study, we sought to understand how IL-10 deficiency alters macrophage programming and specifically for IMs, bacterial tolerance. We hypothesized that the lack of IL-10 may alter the chromatin landscape in macrophages changing how they respond to bacteria. We thus determined changes in chromatin accessibility in response to bacteria genome wide in IMs and BMMs from both WT and *Il10*$^{-/-}$ mice.

Results

To investigate how IL-10 deficiency alters macrophage programming and response to bacteria, we studied changes in chromatin accessibility and gene expression induced by bacteria in two types of macrophages from WT or *Il10*$^{-/-}$ mice: bone marrow derived (inflammatory in WT) and intestinal (non-inflammatory in WT). BMMs were treated for 4 h with either lipopolysaccharide (LPS), a molecule found in the outer membrane of bacteria and known to illicit a strong immune response (stimulated; "+LPS"), or phosphate-buffered saline (unstimulated; "−LPS"). IMs were assayed from mice raised GF (no bacteria present") or CR (bacteria present). Due to the small population of cells and expected chromatin effects that are distal from genes [4–6], we measured chromatin accessibility using FAIRE-seq (Formaldehyde-Assisted Isolation of Regulatory Elements followed by high-throughput sequencing) [13], and annotated accessible chromatin using publically available ChIP-seq data from WT BMMs [4–6]. Transcriptional changes were also detected using RNA-seq (Fig. 1A).

LPS and IL-10 regulate three distinct classes of differentially accessible chromatin

We first studied BMMs, where changes in histone modifications and transcription factor binding reflective of the inflammatory response have been studied in WT cells [4–6]. The effect of IL-10-deficiency on chromatin and gene expression in BMMs is unknown, though they exhibit an exaggerated inflammatory response to bacteria [11, 14].

We distinguished genomic regions with accessible chromatin selective to IL-10 status or LPS stimulation and classified 9,457 300-bp intervals into three categories by hierarchical clustering (Fig. 1B, Supporting Information Fig. 1A). One class exhibited increased chromatin accessibility upon LPS stimulation ("inducible"; e.g., *Nos2* promoter, Fig. 1C), and another demonstrated reduced chromatin accessibility upon LPS stimulation ("reducible"; e.g., *Tcf12* intron, Fig. 1D). In the third category, chromatin was at baseline more accessible in *Il10*$^{-/-}$ BMMs and accessibility was exaggerated following stimulation (e.g., *Tle4* promoter, Fig. 1E). We denoted this third class as IL-10 variable accessible regions (IL10VARs) since IL-10 deficiency drove the observed variable chromatin profile. The majority of sites were considered inducible (5,579; 59%), with fewer in the IL10VAR (2,883; 30%) and reducible (995; 11%) classes.

To annotate these three differential chromatin classes, we first tested their association with histone modifications found in active promoters and enhancers (H3K27ac, H3K4me1, H3K4me3) as well as occupancy of AP-1 and ETS family transcription factors (JunB, PU.1), other immunomodulatory transcription factors (Bcl6 and NF-κB), and RNA polymerase II (RNA Pol II) (Fig. 1F). These data were derived from recent studies of the chromatin-mediated response to LPS stimulation in WT BMMs [4–6]; *Il10*$^{-/-}$ BMMs were not considered in this work. Inducible and reducible sites showed concordant and dramatic changes in H3K27ac, JunB, and PU.1 binding upon stimulation, indicating that LPS-responsive regions gain or lose hallmarks of active enhancer elements. Interestingly, IL10VARs exhibited increased recruitment of JunB upon LPS stimulation, whereas H3K4me3, H3K27ac, and PU.1 signals remained enriched but unchanged, at least in WT BMMs.

To extend these results to the *Il10*$^{-/-}$ BMMs, we performed H3K27ac ChIP-qPCR at three exemplary IL10VAR loci and one control locus in both WT and *Il10*$^{-/-}$ cells (Supporting Information Fig. 1B and C). For two of these regions, H3K27ac was present in WT cells but enhanced in *Il10*$^{-/-}$ cells, as predicted by our FAIRE data. Further, we found that an inaccessible region devoid of H3K27ac in WT cells exhibited both accessible chromatin by FAIRE and robust H3K27ac in *Il10*$^{-/-}$ cells. Together these data indicate that changes in accessible chromatin associated with the lack of IL-10 can directly coincide with changes in histone modifications.

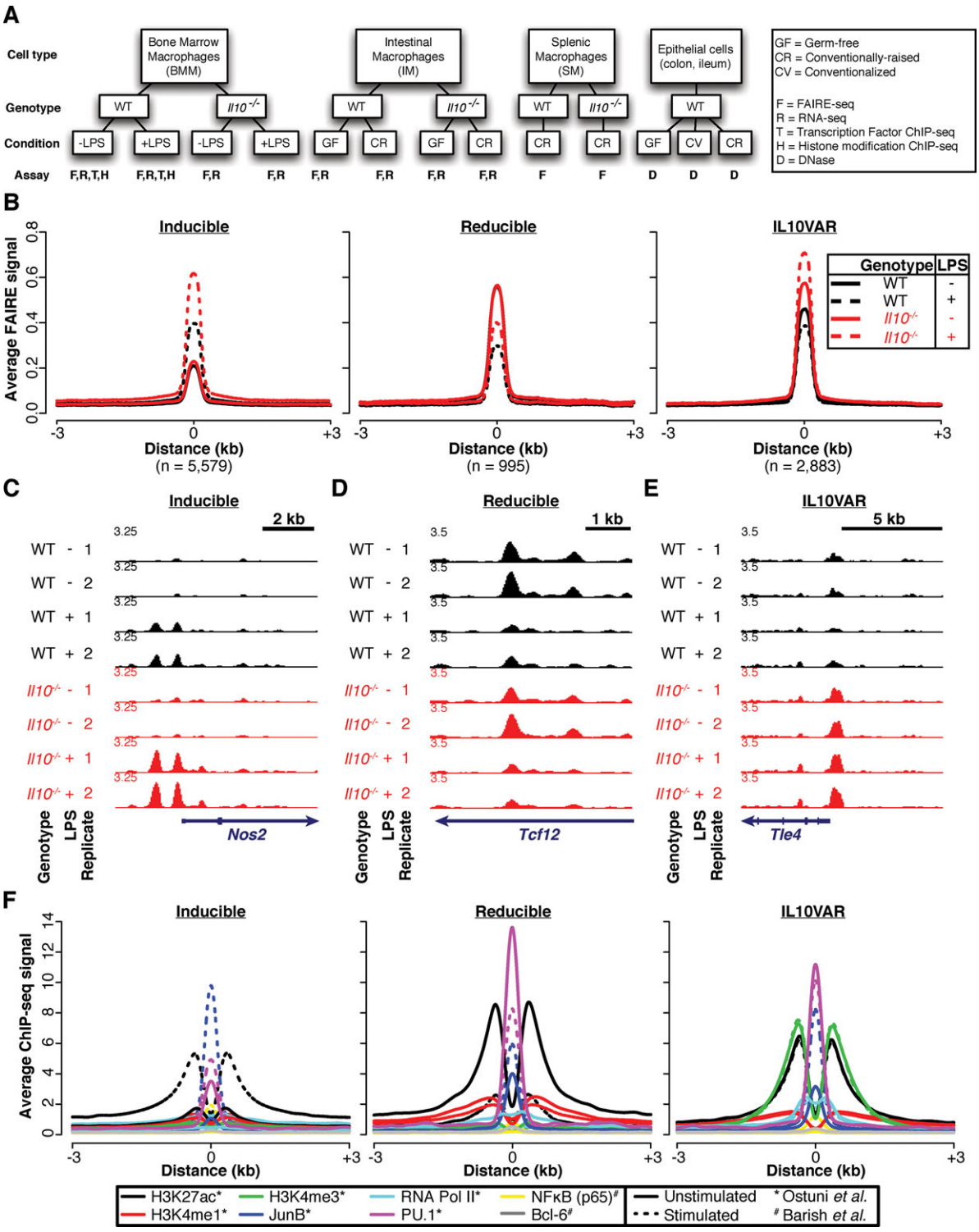

Figure 1. Three regulatory element classes in BMMs driven by IL-10 deficiency and bacterial stimulation. (A) Experimental setup. BMMs were isolated from WT and *Il10*$^{-/-}$ mice in biological duplicate, with one animal per replicate. BMMs stimulated with LPS were compared against unstimulated control (-LPS). IMs were isolated from the lamina propria intestinal layer of WT and *Il10*$^{-/-}$ mice in biological duplicate or triplicate. IMs isolated from GF mice (four animals pooled per replicate) were compared against CR mice (two animals pooled per replicate). FAIRE data were also similarly generated on WT and *Il10*$^{-/-}$ CR splenic macrophages using pools of two animals per replicate. (B) Average normalized FAIRE-seq signal across two biological replicates (one animal per replicate) for WT (black) and *Il10*$^{-/-}$ (red) for both LPS-stimulated (dotted) and control (solid) BMMs are plotted around regions (±3 kb) classified as inducible (left), reducible (middle), or IL10VAR (right). (C–E) Representative loci for inducible (C), reducible (D), and IL10VARs (E). (F) Annotation with published ChIP-seq signal [4–6].

We next searched for overenriched transcription factor motifs. All three classes were enriched with similar frequency for the PU.1 motif (Supporting Information Fig. 1D). The NF-κB motif was selective to the inducible class, whereas the AP-1 motif was found in both inducible and IL10VARs (Supporting Information Fig 1D). These results further support the transcription factor occupancy associations based on ChIP-seq data (Fig. 1F) and identify PU.1 as a factor in all three classes. PU.1 is a known master regulator driving transcriptional responses in macrophages, and along with other transcription factors establishes tissue-specific characteristics of macrophage populations [15].

To determine whether each differential chromatin class targeted functionally related genes, we mapped chromatin regions to genes and searched for enriched pathways using Genomic Regions Enrichment of Annotations Tool (GREAT) [16], independent of underlying gene expression (Supporting Information Fig. 1E). The inducible class was enriched for pathways related to immune response and LPS-responsive genes, and others linked to chemokine and cytokine signaling, including *Il12a, Il18, Ccl2–4, Ccr1–3, Ccr7,* and *Ccr9*. Reducible regions were linked to genes implicated in leukocyte activation, and IL10VARs were linked to FoxP3 and Myc targets. Taken together, these data show that FAIRE-seq detects active regulatory elements in multiple classes linked to biologically meaningful pathways [17, 18].

Lastly, we determined whether chromatin alterations were concordant with gene expression changes in the same BMMs. First, independent of chromatin status, we found 2,715 genes upregulated and 1,496 downregulated by LPS in WT mice (adjusted $p < 1\times10^{-5}$; Fig. 2A), many of which are integral to macrophage biology (Fig. 2B) [19]. Next, to link changes in chromatin accessibility to expression changes driven by LPS and IL-10 deficiency, we associated regions in the three chromatin classes to genes using GREAT [16], then computed the fraction of those genes more highly (positive $\log_2$ fold-change) or lowly (negative $\log_2$ fold-change) expressed due to LPS stimulation or IL-10-deficiency (Fig. 2C). Unexpectedly, we found a nearly equal proportion of down-regulated and up-regulated genes linked to the inducible class upon LPS stimulation. Subdividing these up- and down-regulated genes, we observed that their promoters showed differential H3K27ac and RNA Pol II levels, with increasing H3K27ac enrichment coinciding with increasing gene expression (Supporting Information Fig. 1F). Furthermore, genes linked to inducible chromatin sites whose expression increased upon LPS stimulation consisted of canonical cytokine signaling pathway members, whereas those with decreased expression included known anti-inflammatory mediators, such as *Mef2c, Mef2d, Cx3cr1, IL6r,* and *Myc*. Mef2d directly mediates IL-10 expression levels[20], and Myc is a critical transcription factor for many cellular functions, including anti-inflammation in macrophages[18]. In contrast to these dichotomous inducible chromatin sites, genes linked to reducible sites and IL10VARs tended to show decreased expression (Fig. 2C). Together, these data indicate that LPS stimulation tends to more frequently increase chromatin accessibility, but results in decreased expression of more genes. Our findings highlight the highly dynamic nature of macrophage chromatin accessibility regulated by cytokines and bacterial products, in agreement with recent studies[6]. It also suggests recruitment of both transcriptional activators and repressors to accessible chromatin, such as has been shown during macrophage differentiation[21]. Furthermore, these results suggest that IL-10-deficiency leads to baseline chromatin accessibility changes that may poise chromatin for recruiting transcription factors that drive the transcriptional differences and increased inflammation in these mice.

Il10$^{-/-}$ IMs exhibit chromatin changes mimicking inflammation

In contrast to macrophages from other organs, IMs under physiological conditions efficiently eradicate microbes that breach the intestinal epithelial barrier without mounting a potent inflammatory response. Mechanisms governing these functional adaptations of IMs, however, remain incompletely elucidated, and the loss of this bacterial tolerance underlies chronic intestinal inflammatory diseases.

As with BMMs, we hierarchically clustered 7,957 300-bp regions with variable chromatin accessibility based on IL-10 status (WT vs. *Il10*$^{-/-}$) and presence of bacteria (GF vs. CR) in macrophages isolated from the lamina propria layer of the intestine (>95% purity, Supporting Information Fig. 2A). Similar to BMMs, we observed three distinct categories (inducible, reducible, and IL10VAR) (Supporting Information Fig. 2B, Fig. 3A–B), however with markedly different proportions; the majority (4,724, 59%) were classified as IL10VARs, whereas in BMMs the majority (5,579, 57%) were inducible elements (Supporting Information Fig. 1A, Fig. 1B). Importantly, IM IL10VARs were characterized by altered chromatin accessibility in *Il10*$^{-/-}$ mice even in the absence of intestinal bacteria and whose resulting chromatin landscape strongly mimicked that displayed by LPS-stimulated BMMs. We thus hypothesized that chromatin and transcriptional changes driven by IL-10-deficiency in IMs heavily contribute to an inflammatory response typically seen in BMMs, but not IMs (Fig. 3B–D, Supporting Information Fig. 2C).

We investigated similarities between IM IL10VARs and LPS-responsive (inducible) regions in BMMs in several ways. First, we determined that 20% of IM IL10VARs directly overlapped BMM inducible regions (Fig. 3C). Linking these regions to genes (GREAT), this concordance increased to 54% of genes held in common (Fig. 3D). Given this overlap, many significantly enriched pathways associated with IM IL10VARs matched those enriched in the BMM inducible class, including cytokine and chemokine signaling, known perturbation by LPS, and known immune system functions (Supporting Information Fig. 2D). Furthermore, transcription factor motifs found within IM IL10VARs were highly consistent with those in BMM inducible regions, including AP-1, PU.1, CREB, RUNX, and IRF1 (Supporting Information Fig. 2E and 1D).

We next examined gene expression patterns of IMs both confined to the cytokine pathway (Supporting Information Fig. 3A) as well as globally (Supporting Information Fig. 3B and C). We

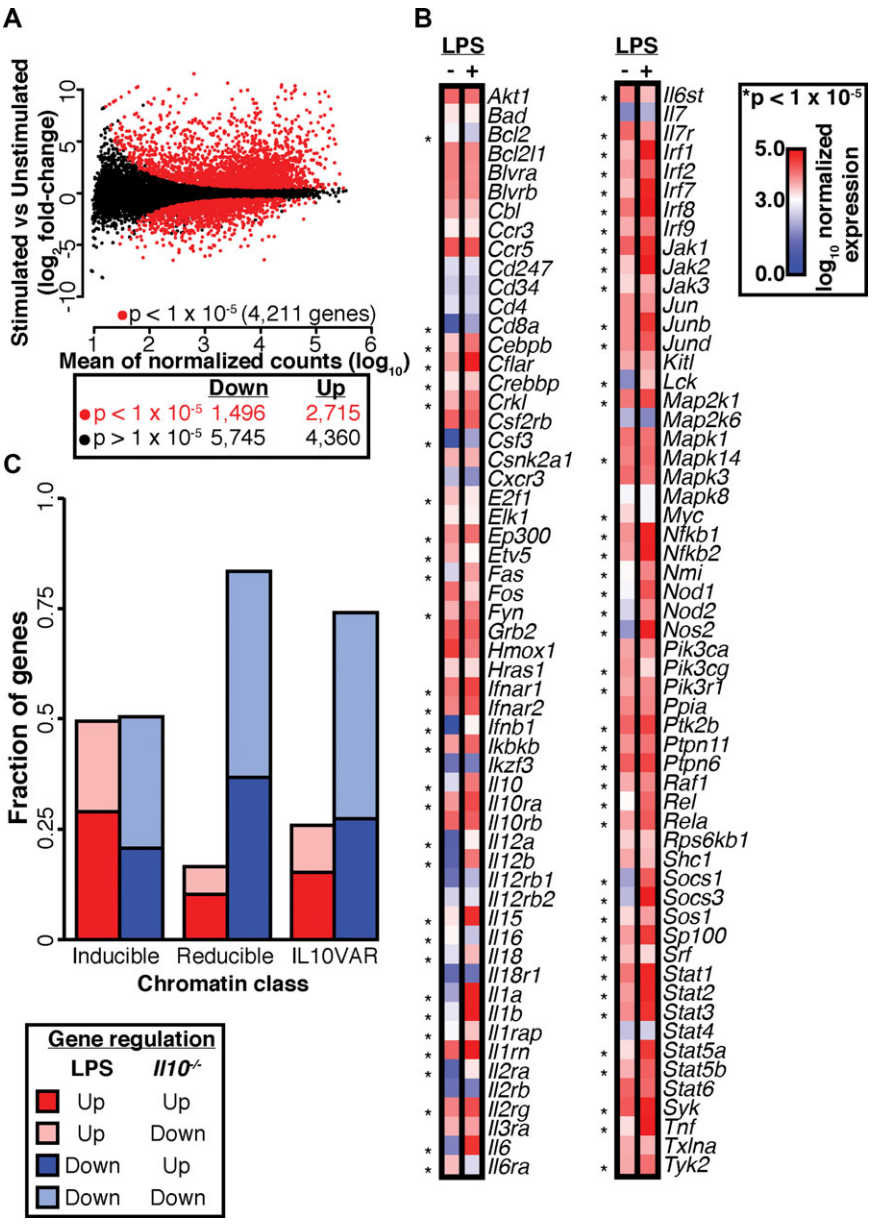

Figure 2. Alterations in gene expression due to IL-10 status or bacterial stimulation affect many key cytokine genes. (A) Differential expression analysis performed using DEseq between LPS-stimulated and unstimulated BMMs for two biological replicates (one animal per replicate; red points, adjusted $p < 1 \times 10^{-5}$). (B) Log_{10} expression of genes in the cytokine signaling pathway is plotted on a scale of 0 (blue) to 3.0 (white) to 5.0 (red). Differentially expressed genes (determined by DEseq; adjusted $p < 1{\times}10^{-5}$) are denoted with an asterisk. (C) Fraction of genes linked to three regulatory element classes that were up- or downregulated with respect to IL-10 status ($Il10^{-/-}$ vs. WT) or LPS stimulation.

noticed that although the baseline expression pattern was altered in GF IMs from $Il10^{-/-}$ mice, unlike at the chromatin level, it did not mimic LPS-stimulated WT BMMs. Instead, this expression phenotype was only apparent in IMs from CR $Il10^{-/-}$ mice, where the aberrant inflammatory response is manifested [8, 11, 14, 22]. For example, nearly all interleukin genes exhibited a relative expression decrease at baseline in GF $Il10^{-/-}$ IMs, but were massively upregulated in CR $Il10^{-/-}$ IMs (Supporting Information Fig. 3A). When comparing gene expression globally, IL-10-associated expression changes in IMs correlated more strongly with expression changes in BMMs driven by stimulation ($r = 0.15$) than with those driven by IL-10 deficiency in BMMs ($r = 0.1$; Supporting Information Fig. 3B). However, only the CR IMs from $Il10^{-/-}$ mice displayed a high similarity to LPS-stimulated BMMs with respect to these gene expression changes (Supporting Information Fig. 3C).

Together, our findings suggest that IL-10-deficiency alone is sufficient to poise IM chromatin for an inflammatory response to intestinal bacteria, even before microbial colonization and subsequent manifestation of inflammation. This raises the possibility that in the absence of IL-10, IMs lose their hyporesponsiveness to the intestinal bacteria and acquire a chromatin accessibility pattern consistent with LPS-stimulated BMMs, poising cells to respond inappropriately through unabated intestinal inflammation. This model is supported by well-described phenotypic differences between intestinal and non-IMs [3, 14, 19, 23, 24]. However, our data suggest chromatin is a key mediator of this microbial response.

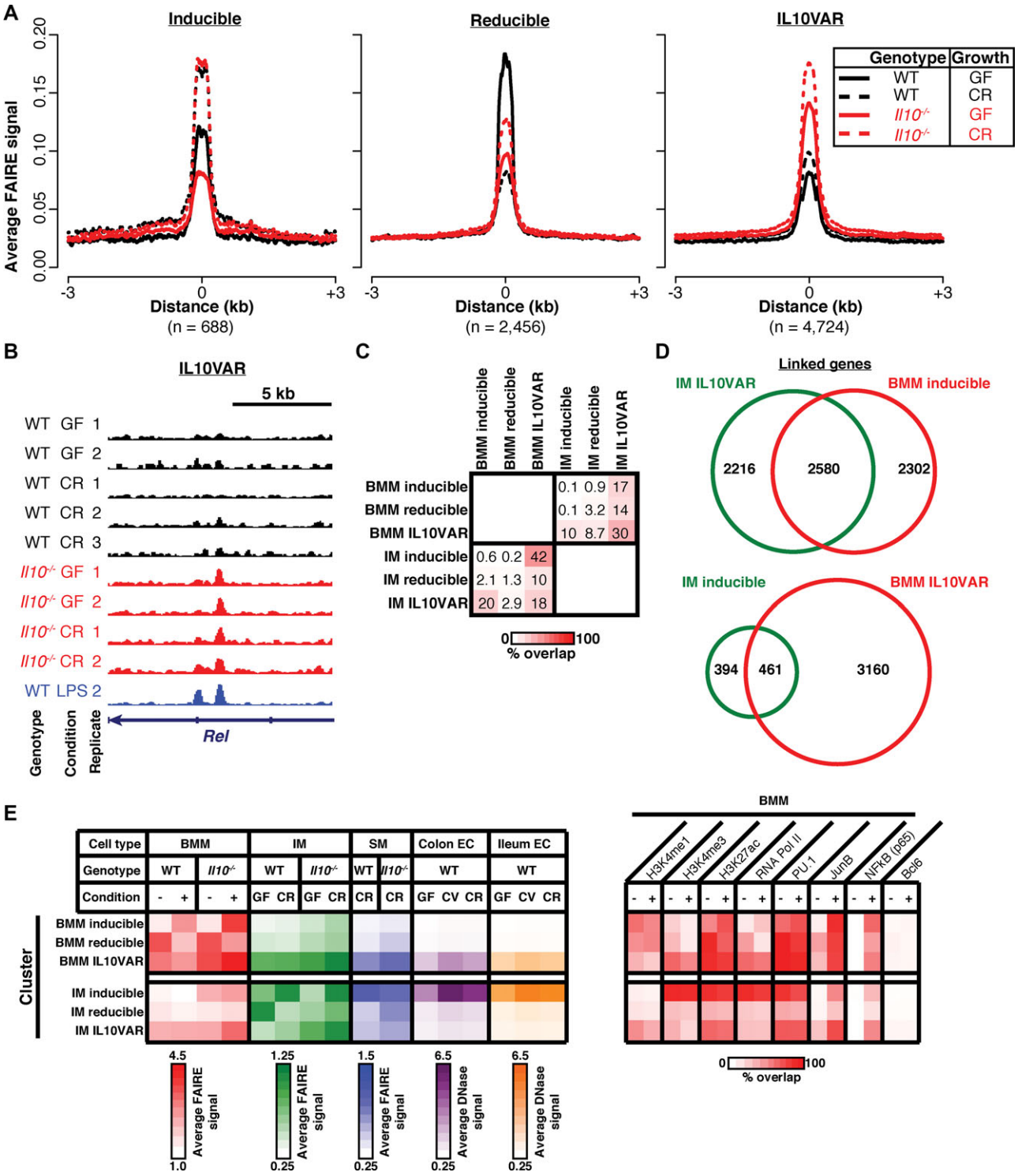

Figure 3. Aberrant chromatin accessibility in *Il10*$^{-/-}$ IMs from GF mice mimics that of LPS-stimulated BMMs but is not cell type specific. (A) Average normalized FAIRE-seq signal across two to three biological replicates for WT (black) and *Il10*$^{-/-}$ (red) for both CR (dotted; two animals pooled per replicate) and GF (solid; four animals pooled per replicate) IMs is plotted around regions (±3 kb) classified as inducible (left), reducible (middle), or IL10VARs (right). (B) Representative locus for IL10VARs. FAIRE-seq signal from WT LPS-stimulated BMMs (blue) included as a comparator for IL10VARs. (C) Percentage of overlapping sites in three regulatory element classes from BMMs and IMs. Overlap values presented reflect the percentage overlap relative to the given set of regions on the left. (D) Fraction of common genes linked to IM IL10VAR and BMM inducible (top) or IM inducible and BMM IL10VAR (bottom). (E) Annotation of regulatory element classes with averaged FAIRE-seq signal in BMM (red), IM (green), and splenic macrophages (blue; two animals pooled per replicate), as well as published DNase-seq signal from colonic (purple) and ileal epithelial cells (orange). Summarized ChIP-seq data for transcription factors and histone modifications are presented on the right as percent overlap.

Regions of dynamic macrophage chromatin are associated with enhancers but are not cell type specific

Camp et al. [25] recently described changes in chromatin accessibility and gene expression in intestinal (colonic and ileum) epithelial cells of CR and GF mice, and GF mice intentionally conventionalized with the intestinal bacteria. They reported few significant accessibility changes with bacterial colonization. We questioned whether differential chromatin regions in macrophages exhibited altered chromatin accessibility in epithelial cells. In addition, we wondered whether IL-10 deficiency driven alterations in chromatin were observed in macrophages from other organs. For the latter, we therefore generated and assessed chromatin accessibility data in splenic macrophages from the same CR mice described above as an in vivo control of macrophage cellular environment. We integrated these chromatin data with the occupancy of histone modifications (H3K27ac, H3K4me1, and H3K4me3) and transcription factors (PU.1, JunB, NF-κB, Bcl6, and RNA polymerase II [RNA Pol II]) in BMMs in the presence or absence of LPS to more comprehensively annotate the macrophage regulatory landscape (Fig. 3E). We found that IL-10-deficiency also altered the baseline chromatin accessibility of splenic macrophages, suggesting similar regulatory defects in the absence of basal IL-10 production. Interestingly, inducible sites in IMs (almost half of which overlap BMM IL10VARs, Fig. 3C) also exhibited changes in epithelial cells isolated from WT GF mice compared to CR and conventionalized mice, suggesting these bacteria-responsive dynamic regions may not be cell type specific. Based on consistent PU.1 occupancy in the presence or absence of LPS stimulation in all IM and BMM differential chromatin regions, our data suggest that PU.1 may recruit proinflammatory (AP-1, NF-κB) factors necessary to facilitate the bacterial response, a model that has been previously proposed [5, 6].

Chromatin alterations may also occur in human CD

As shown above (Fig. 3), IL-10 deficiency sufficiently poised IM chromatin for an inappropriate inflammatory response even in the absence of intestinal bacteria. We wondered whether specific sites of chromatin alterations identified here were representative of changes associated with loss of macrophage tolerance in humans as well. We focused on IL10VARs in IMs to assess specifically those sites linked with genetic variation. To test the conservation of chromatin changes in human CD, we generated FAIRE-seq data from colonic mucosal biopsies from two CD and two control patients. These patients were genotyped and did not harbor variants near *IL10* or *IL10RB* previously linked with CD [26] and had no differences in IL-10 expression as measured by RNA-seq on the same colonic mucosal tissue samples (Fig. 4A). We next converted the coordinates of the 4,724 IM IL10VARs over to the reference human genome. As genomic regulatory regions can change location during evolution [27], we evaluated 300-bp windows within a 10 kb region centered around the midpoint of each mapped regulatory element for changes in FAIRE signal between CD and control colon samples. We found 327 windows with differential FAIRE signal, a significant enrichment relative to random chance (permutation, $p < 0.001$; Fig. 4B). Of these, 304 (93%) exhibited increased accessibility in CD patients. This significant linkage between syntenic human–mouse regions was not unique to IL10VARs, however, and was also seen for inducible and reducible classes as well (Fig. 4B). As a class, syntenically mapped IL10VARs were again significantly enriched near key cytokine pathway and proinflammatory genes, including *IL7R* (Fig. 4C–D), *NFKB1, MYD88*, as well as a component of Mediator, *MED19*. These sites and others suggest that human CD patients may also have chromatin alterations associated with an inappropriate immune response.

One interesting site demonstrated CD selectivity, overlapped a site of genetic heterogeneity, and was upstream of the interleukin-7 receptor gene (*IL7R*; Fig. 4C and D). One CD patient was heterozygous at rs185659576, a T/C variant not previously reported to have disease relevance, whereas the controls and other CD patient were homozygous for the T allele. We tested for allelic effects on protein binding by using biotin-labeled probes surrounding the C or T alleles, incubated with human monocyte (THP-1) nuclear lysate and subjected to electrophoretic mobility shift assays (EMSAs; Fig. 4E). Band shifts indicative of multiple complexes were observed. Moreover, a protein complex (Fig. 4E, arrow) was observed when the C allele was present but not the T allele, suggesting differential protein binding dependent on the rs185659576 allele. Competition of labeled C-allele probe with excess unlabeled C-allele probe more efficiently competed away allele-specific bands than excess unlabeled T-allele probe, demonstrating allele-specificity of the protein–DNA complexes. Together, these data suggest that an unknown transcriptional regulator binds preferentially to the rs185659576-C allele in monocytes. Collectively, these results provide a proof-of-concept for using chromatin accessibility important in IM biology and colitis pathogenesis to identify and prioritize regions for further experimental investigation that may be directly driving susceptibility to human CD.

Ectopic IL-10 supplementation minimally affects aberrant chromatin associated with IL-10 deficiency

The spontaneous onset of intestinal inflammation in *Il10*$^{-/-}$ mice may be reversed by treatment with recombinant IL-10 soon after weaning [28]. Exogenous IL-10 also attenuates the proinflammatory transcriptional output in BMMs. However, use of recombinant IL-10 for the treatment of CD has been largely unsuccessful [29] with little understanding for the basis of this failure. IL10VARs exhibited increased chromatin accessibility at baseline and were associated with expression changes in key inflammation-related genes in response to microbial stimulation (Figs. 1 and 3, Supporting Information Figs. 2–3). To investigate whether IL-10 supplementation in vitro can revert the *Il10*$^{-/-}$ BMM chromatin profile to a normal state, we performed FAIRE-seq on *Il10*$^{-/-}$ BMMs stimulated with IL-10 and/or LPS. Surprisingly, chromatin accessibility

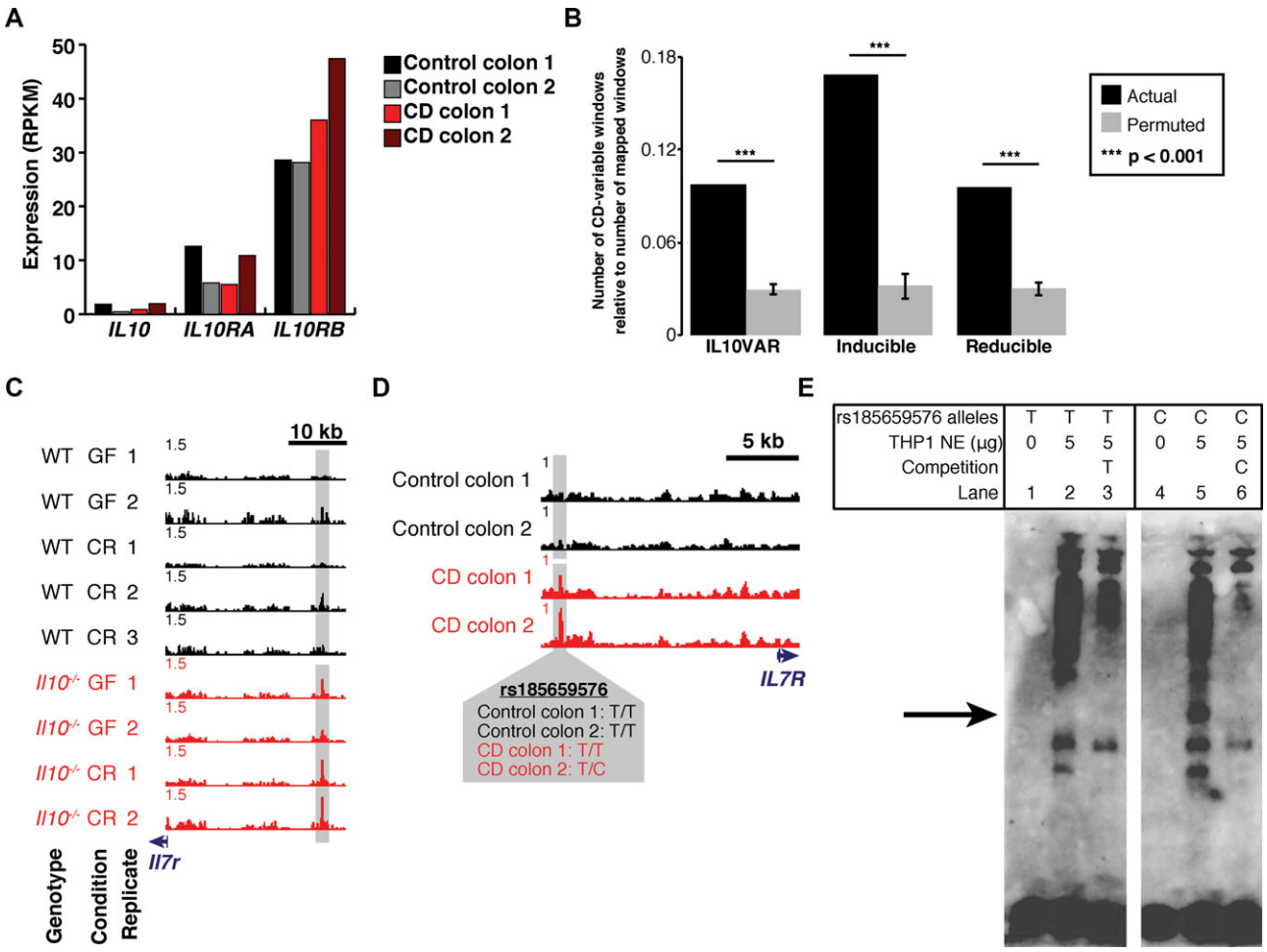

Figure 4. IL10VARs display enrichment for differential chromatin in syntenic regions in human tissue and allele specific protein binding. (A) Expression levels (RPKM) of *IL10*, *IL10RA*, and *IL10RB* for human patients (two control, two CD) biopsied as measured by RNA-seq. (B) Regions falling into one of three regulatory element classes from IMs were mapped to the human genome and selected based on CD-selective chromatin accessibility in mucosal biopsies from two CD and two non-CD patients. The number of final CD-variable windows relative to the number of windows that successfully mapped to the human genome is compared to a permuted control for each regulatory element class. *P*-values were derived empirically based on 1,000 permutations. Error bars represent SD around the mean. (C–D) Normalized FAIRE-seq signal at *Il7r* (mouse, C) and *IL7R* (human, D) depicting conserved enrichment in mouse IMs and human mucosal biopsies. CD and control patient genotypes for overlapping variant rs185659576 are also presented. (E) EMSA with human THP-1 monocyte nuclear extract utilizing complementary oligonucleotides containing either the T (reference) or C (alternate) alleles of rs185659576. Protein complex binding specifically to the C allele is demarcated with an arrow.

at <5% of the 2,883 IL10VARs in BMMs was affected by the addition of IL-10 (Fig. 5), and was unchanged at nearly all genes with known expression changes (data not shown). Chromatin accessibility was also unaffected at reducible regions (Supporting Information Fig. 4A), but was more pronounced at inducible regions (Supporting Information Fig. 4B), with a small subset near genes with IL-10-mediated expression changes. These data suggest IL-10 may transiently modulate expression and chromatin structure of certain target genes (e.g., *Irf1*, Fig. 5B); however, at most IL-10-dependent loci, exogenous IL-10 does not significantly remodel chromatin. We propose that the absence of IL-10 during development drives the formation of a chromatin landscape that leads IMs to respond aberrantly to bacterial stimulation that cannot be corrected by IL-10 after differentiation. This model is supported by the development of early and severe CD in patients with genetic dysregulation of IL-10 signaling [30], the lack of therapeutic response to recombinant IL-10 [29], and increased success with earlier IL-10 therapeutic intervention[28].

Discussion

Chromatin accessibility influences cellular identity, providing access for transcription factors and setting the stage for responses to changing cellular conditions and external stimuli. For each cell, the chromatin landscape evolves throughout differentiation [31–34], finely tuning regulatory programs. Closely related cells, such as macrophages from different tissues, will share a large fraction of their accessible regions associated with common functions, but their differences highlight unique regulatory programs driven by their environments and their normal responses. This was demonstrated in a recent study showing macrophage gene

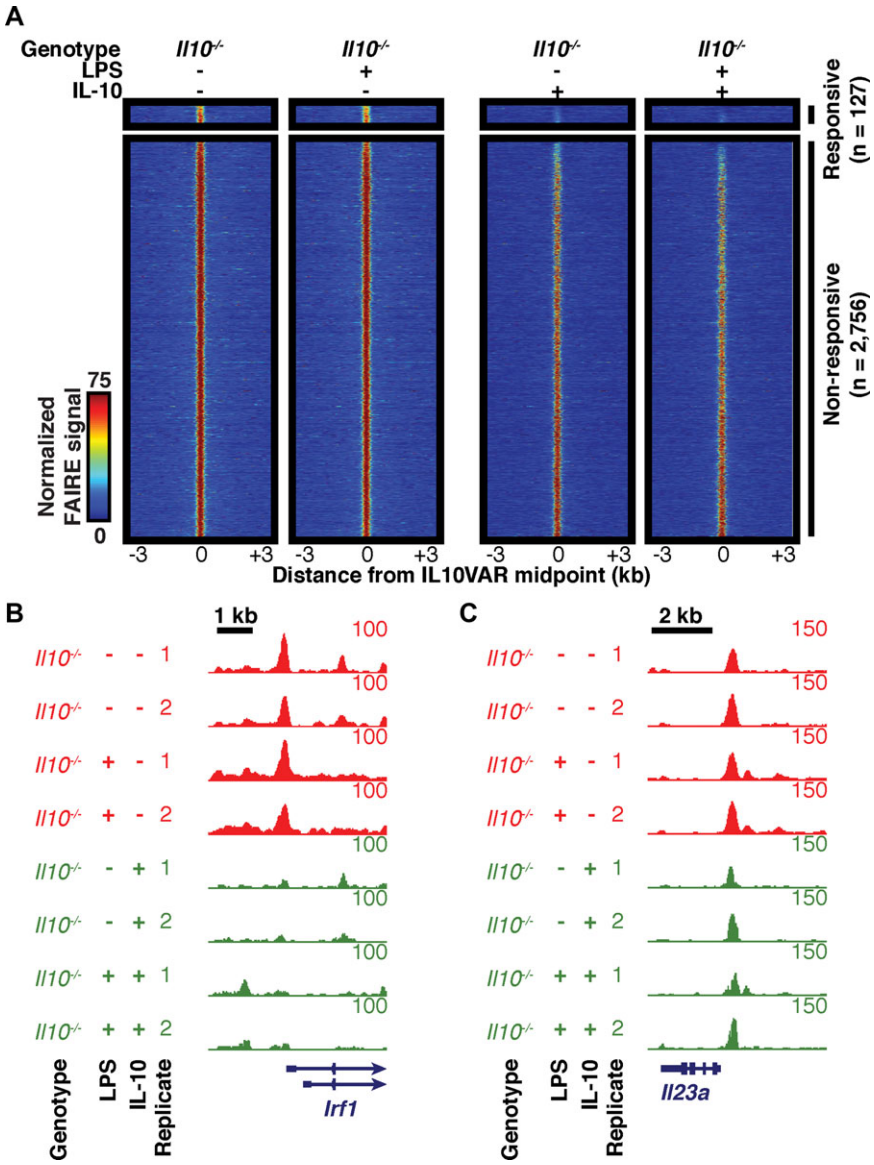

Figure 5. Ectopic IL-10 does not revert aberrant baseline chromatin structure of *Il10*$^{-/-}$ BMMs. (A) Normalized FAIRE-seq signal for BMMs with and without LPS stimulation and ectopic IL-10 supplementation within 3 kb of IL10VARs divided into responsive or nonresponsive based on effect from ectopic IL-10. Each experiment was performed in biological duplicate (one animal per replicate), and signals were averaged across replicates. (B–C) FAIRE-seq signal without (red) and with (green) ectopic IL-10 at responsive (B) and non-responsive (C) regions.

expression and chromatin differences depending on the microenvironment [35], despite a common progenitor [36]. Further, Lavin et al. showed that the differentiated macrophage chromatin landscape could be reprogrammed after changing the microenvironment. This is likely due, at least in part, to the tissue-restricted expression of critical transcription factors that govern tissue macrophage function, including members of the GATA, RUNX, and MEF2 families [35]. Microenvironment and tissue-restricted transcription factors therefore likely play prominent roles in properly establishing chromatin during differentiation through subtle alterations of the common canvas in progenitor cells, leading to significantly different behaviors, a concept proposed in a study of chromatin during *Drosophila* development [32].

IMs respond to bacteria very differently compared to macrophages from other tissues. We provide strong evidence here that chromatin plays a critical role in maintaining this cellular identity and function. The establishment of a proper chromatin landscape may depend on IL-10 early in development, even though IL-10 is not known to be a classic chromatin remodeler, pioneer factor, or even a factor that directly interacts with chromatin. We believe this may have relevance for the development of therapies for chronic intestinal inflammatory diseases. Drugs that simply target aberrantly expressed genes may fail if restoration of gene activity does not correct abnormal function due to an improper chromatin environment in which to operate, as is the case with current management strategies for patients with CD [37]. In humans, mutations in IL-10 receptor genes (*IL10RA, IL10RB*) are associated with early, severe CD [30], indicating that IL-10 activity is relevant in human disease, but are rare. Interestingly, clinical trials have explored recombinant IL-10 therapy in CD with little success [29]. Various reasons have been cited for this lack of therapeutic efficacy, including dosage, timing of IL-10 therapy, and resulting IL-10 concentration in the intestine, and the large degree of disease phenotype heterogeneity among patients [38].

Our results suggest an alternative, complementary explanation. If macrophage cellular identity has been stably altered at the chromatin level, simply restoring IL-10 levels may not be sufficient, especially in the long term. More generally, if factors essential for proper chromatin programming during development or differentiation are missing, their lack of chromatin-modifying activity may preclude their efficacy as a sole therapy later in time. This model is supported by a longitudinal study of disease progression in mice, where recombinant IL-10 therapy administered to weanlings prevented the onset of intestinal inflammation, whereas adult mice only modestly exhibited reduced progression [28]. Future studies can examine macrophage chromatin dynamics during development. However, proper temporal expression of critical tissue-specific transcription factors and other genes is also likely to play a role in establishing appropriate cellular identities during differentiation, and may very well occur upstream of structural changes to chromatin.

We also believe that this has important implications for how underlying genetics should be investigated for contributions to disease, and importantly here chronic intestinal inflammatory diseases. Not only should variant effects be investigated in the end disease cell, but also how they may contribute the establishment of the epigenetic program. In complex human disease, contributions from multiple genetic variants may result in subtle chromatin changes that when combined with other environmental factors may be principal drivers behind increased disease susceptibility. Genetic predisposition to intestinal inflammation, regardless of whether IL-10 signaling is involved, may therefore result from a poised chromatin state that drives an aberrant transcriptional response to stimuli in a tissue-specific context. Neither human CD patients we analyzed had genotypes that indicated IL-10 signaling had been affected, yet they exhibited chromatin changes similar to those found in our *Il10*$^{-/-}$ mouse colitis models. These findings support the well-described differences in transcriptional responses to microbial stimulation between IMs and other non-IM populations [2, 39]. Loss of this perpetual hypo-responsiveness to the intestinal bacteria is also observed in IMs from patients with CD compared to IMs from control patients [3].

We found that IL-10 deficiency can profoundly influence establishment of the proper macrophage chromatin environment, effectively altering cellular identity resulting in aberrant behavior. We found that in the presence of bacteria, *Il10*$^{-/-}$ IMs adopted chromatin and gene expression patterns characteristic of an inflammatory response. In *Il10*$^{-/-}$ mice raised GF, which do not exhibit intestinal inflammation, chromatin accessibility patterns indicative of inflammation were also present but lacked the corresponding gene expression changes.

Additionally, our work shows an association between sites in mice reflective of a baseline alteration in chromatin driven by IL-10 deficiency and similar CD specific changes in syntenic regions in human colon tissue, despite the fact that the underlying genetic changes are not the same. Based on these results, we postulate that multiple genetic mechanisms may drive a common core chromatin signature reflective of chronic inflammation. It is critical, therefore, to understand how all types of genetic and environmental variation is changing the chromatin landscape leading to increased disease susceptibility.

Our findings also have direct implications for the development of novel therapeutic strategies for CD and possibly other chronic inflammatory diseases that result from a strong interplay between genetics and the environment. Future studies that uncover the mechanisms of regulatory aberrations in chronic inflammatory disorders should direct the exploration of new therapeutic strategies toward stimulation or inhibition of the appropriate intestine-specific macrophage response, especially in macrophages isolated from the healthy and inflamed human intestine.

Materials and methods

Reagents, mice, and macrophages

IL-10 was purchased from BD PharMingen (San Diego, CA), LPS was obtained from Sigma-Aldrich (St. Louis, MO). WT and *Il10*$^{-/-}$ mice on a C57BL/6 background and controls were purchased from The Jackson Laboratory (Bar Harbor, ME). WT and *Il10*$^{-/-}$ mice on the C57BL/6 background were matched for age in all experiments. GF mice (WT and *Il10*$^{-/-}$) were derived by embryo transplant and maintained at the National Gnotobiotic Resource Center at the University of North Carolina. Mice were housed in accordance with guidelines from the American Association for Laboratory Animal Care and Research Protocols, and the Institutional Animal Care and Use Committee of the University of North Carolina approved experiments (IACUC #12-199).

Macrophage isolation and stimulation

Bone marrow derived macrophages (BMMs) were harvested, cultured, and stimulated as described [11] in biological duplicate (one animal per replicate). Macrophages were stimulated with 100 ng/mL LPS where denoted. For *Il10*$^{-/-}$ macrophages supplemented with IL-10, cells were pretreated with IL-10 (10 ng/mL) for 24 h. Lamina propria mononuclear cells (here "IMs") were isolated from mouse colon by an enzymatic method and density gradient centrifugation, as described previously [40]. Splenic macrophages (here "SMs") were isolated as previously described [41]. Lamina propria mononuclear cells and splenocytes were further separated into CD11b^{+} cells using anti-CD11b microbeads (Miltenyi Biotec, Auburn, CA). Purity was >90% by flow cytometric analysis (Supporting Information Fig. 2A). IMs and SMs were analyzed in biological duplicate or triplicate as indicated; two littermate animals were pooled for CR experiments, and four littermate animals were pooled for GF experiments.

Creation of a mouse genome blacklist filter

Certain types of genomic regions are known to induce artifactual signal caused by experimental or technical biases, and thus

Table 1. Primer sequences used for quantitative PCR

Primer set name	Forward	Reverse
Suz12	5′TGGTGGGGGAGTTAAATATCTG	5′ATGACAGGTGCTTTTGAGGTTT
Irf1	5′GAGTTCCTACTGCCCCGTATTT	5′TATGTCCCTGTACCGCCTTACT
Steap3	5′CTCAGCAGTTTGTGCTGATAGG	5′GTGCCCTTATCTACCATTTCCA
Cacng8 (neg. control)	5′AGGCCATGTTTGGGATACTG	5′AAAGCAGAAGCGGAACTCAC

it has been suggested that these regions be masked or ignored [42]. Mouse blacklists were therefore created in a fashion consistent with ENCyclopedia Of DNA Elements (ENCODE) [43] for the human genome, including problematic satellite repetitive elements (CENSAT, GSAT, MurSAT, and SYNREP, as defined by RepeatMasker), regions with sequence homology to mitochondrial DNA (NumtS), rRNA, and regions on chrX with strong sequence homology to chrY. The effects of these types of genomic elements on sequencing data has been previously discussed [42].

FAIRE and hierarchical clustering of differentially open chromatin

FAIRE was performed as previously described [13] in biological duplicate or triplicate as indicated. Sequencing was performed using 50-bp single-end reads (Illumina HiSeq 2000). Reads were filtered such that their identical sequence could appear only up to five times, and only reads with quality score greater than 20 for 90% of bases were retained. Reads were then were filtered using TagDust [44] and aligned to the reference mouse genome (mm9) with GSNAP [45] using a k-mer size of 15, indel penalty of 5, and allowing 1 mismatch. Reads aligning to more than four locations or overlapped blacklisted regions of the mouse genome were removed. Reads were counted in 300-bp windows sliding by 100 bp across the genome and normalized for sequencing depth. Windows were then intersected with the union set of the top 50 000 peaks identified for each sample using Fseq [46]. For clustering analyses, only windows with variable signal (row SD $>$ 0.75) were retained. Overlapping windows were handled by retaining the one window for a given region with the maximal SD. Remaining windows were then hierarchically clustered and plotted. Feature intersections were computed using BEDTools [47]. For comparison with exogenous IL-10, quantile normalization of wiggle files was carried out using DANPOS [48]. Regions were split into "responsive" and "nonresponsive" based on whether a peak called in the +IL-10 conditions fell into the union set of the top 50,000 peaks called for all control samples.

Chromatin immunoprecipitation (ChIP) and quantitative PCR

ChIP was performed on both WT and *Il10*$^{-/-}$ with the ChIP-IT Express kit (ActiveMotif, Carlsbad, CA) according to the manufacturer's recommendations. Briefly, 10×10^6 BMMs were washed with complete growth media, and fixed with 1% formaldehyde for 10 min at room temperature. IPs were carried out using a polyclonal H3K27ac antibody (ab4729; Abcam, Cambridge, MA). Real-time PCR was then performed with the SensiFAST SYBR Hi-ROX Kit (Bioline, Boston, MA) as recommended, using primers for the four regions (below); input DNA was diluted tenfold prior to PCR. ChIP enrichment values were compared to input controls and converted to percentage of input DNA immunoprecipitated using $2^{-\Delta Ct}$. These percentage input values were then averaged for three independent biological replicates and SE was computed.

Primer sequences used are shown in Table 1.

Transcript abundance measurements and differential expression using RNA-seq

RNA was isolated using Qiagen RNeasy Mini Kit (Valencia, CA). This kit uses a column-based DNase treatment to eliminate DNA contamination. RNA was sequenced using paired-end 50 bp reads (Illumina Hiseq 2000). Reads were filtered using TagDust (Lassmann et al., 2009 [44]) and only reads with quality score greater than 20 for 90% of bases were retained. Reads were then aligned to the reference mouse genome (mm9) with GSNAP [45] using parameters described above. Reads aligning to blacklisted regions of the mouse genome were removed. Transcript abundance was estimated by computing RPKM [49], using RefSeq gene models aggregated by gene symbol. For differential expression analyses, raw counts over RefSeq exons were used, then compared across samples using DESeq [50] at an adjusted p-value threshold of $p < 1 \times 10^{-5}$.

Analysis of ChIP-seq and DNase-seq data

Sequencing reads were obtained from the Short Read Archive and reprocessed by filtering using TagDust [44] and aligning to the reference mouse genome (mm 9) with Bowtie [51] using default parameters. Reads aligning to blacklisted regions of the mouse genome were removed. Remaining reads were extended in silico to an assumed fragment length of 250 bp. DNase data were obtained from Camp et al. [25].

Motif analysis

Significantly enriched known transcription factor motifs were identified using HOMER [15]. The 300-bp flanking region was

used as local background. The motifs detected de novo are presented in Supporting Information Figures 1 and 2. Highly similar entries were merged.

Ontologies associated with differentially open chromatin

Regions from Clusters 1–3 were associated with Gene Ontologies using GREAT [16]. The top term for a given ontology with $q < 1 \times 10^{-5}$ was presented.

Patient population

CD patients from the adult IBD Center at University of North Carolina were included in this study. A total of four samples (two CD and two non-CD controls, at least 40 mg of tissue each) were studied using FAIRE-seq. This study received IRB approval at UNC Chapel Hill (Protocol # 10–0355).

Genotyping and analysis of human FAIRE-seq data

Genotypes for two non-inflammatory bowel disease and two CD individuals were assayed on the Illumina Immunochip. QC and removal of poor quality SNPs was performed using a standard cluster file from Illumina. Genotype imputation was performed with MaCH-admix [52], and sex-specific, custom genomes were created for each individual using genotype calls for all genotyped and imputed variants. FAIRE-seq reads with quality scores greater than 20 for 90% of bases were retained. High-quality reads were aligned to their respective personalized genomes using the SNP-tolerant GSNAP software [45].

Cross-species analysis

Windows falling into one of the three classes from mouse analyses were converted to coordinates in the human genome using LiftOver with a conservation threshold of 0.1 [27]. These new regions were then extended 5 kb on either side of the region midpoint. New 300 bp windows sliding by 100 bp were then constructed across these 10 kb regions, and normalized FAIRE-seq enrichment for the two control and two CD individuals was computed. Regions with variable open chromatin (row SD > 0.25) were then detected. Overlapping windows were handled by retaining the one window for a given region with the maximal SD. Permutations were computed by shuffling a given class of regions across the uniquely mappable mouse genome, and then repeating this cross-species process 1,000 times and counting how many variable windows were detected relative to the number that converted successfully. *P*-values for permutations were derived empirically based on how many times the shuffled set of mouse windows resulted in more patient-variable regions than the actual regions from our three clusters.

Electrophoretic mobility shift assay (EMSA)

Complementary oligonucleotides (5′-CTTATATATGTAA [C/T]ATATG-3′) were designed around the variant rs185659576 (Integrated DNA Technologies, Coralville, IA). Total nuclear protein of human monocyte THP-1 cells was extracted using a NE-PER Extraction Kit (Thermo Scientific, Waltham, MA), and the protein concentration was measured with the BCA Protein Assay (Thermo Scientific). The LightShift Chemiluminescent EMSA Kit (Thermo Scientific) was used following the manufacturer's protocol, and all incubations were carried out at room temperature. The biotin-labeled probe-protein binding reaction was incubated for 25 min and contained: 1× binding buffer, 1 μg poly(dI-dC), 5 μg nuclear extract, and 200 fmol 5′-biotin-labeled double-stranded oligonucleotide probe in a final 20 μL reaction volume. The unlabeled probe-protein competition reaction contained 100-fold excess of unlabeled probe and was incubated with the nuclear extract for 15 min prior to adding the biotin-labeled probe and incubating for another 25 min. The DNA–protein complexes were resolved using 6% DNA retardation electrophoresis gels (Life Technologies, Carlsbad, CA) in 0.5× TBE (Tris/Boric Acid/EDTA buffer; Lonza, Basel, Switzerland). The gels were transferred to Biodyne Nylon Transfer Membranes (Thermo Scientific). After UV crosslinking, chemiluminescence was used to visualize the protein-probe complexes.

Acknowledgments: We thank J. Rawls and J. Camp for advice and assistance with their published data from epithelial cells, as well as members of the Furey and Sheikh laboratories, D. McKay, and S. Pott for insightful comments. This work was supported by American Gastroenterological Association (AGA) Research Scholar Award (SZS), Broad Medical Research Program (SZS), Crohn's and Colitis Foundation of America's Career Development Award (SZS), and Microbiome Consortium (RBS), R01-ES024983 from NIEHS (MW, SZS and TSF), R01-DK072193 and R01-DK093757 from NIDDK (KLM), P01-DK094779 from NIDDK (RBS and SZS), P40-OD101995 from NIH (RBS), P30-DK034987 from NIDDK (RBS and SZS), and SHARE from the Helmsley Trust (RBS). All data have been deposited to GEO under accession number GSE70517.

Conflict of interest: The authors declare no commercial or financial conflict of interest.

References

1 **Sartor, R. B.**, Microbial influences in inflammatory bowel diseases. *Gastroenterology* 2008. **134**: 577–594.

2 **Sheikh, S. Z. and Plevy, S. E.**, The role of the macrophage in sentinel responses in intestinal immunity. *Curr. Opin. Gastroenterol.* 2010. **26**: 578–582.

3 **Kamada, N., Hisamatsu, T., Okamoto, S., Chinen, H., Kobayashi, T., Sato, T., Sakuraba, A. et al.**, Unique CD14 intestinal macrophages contribute to the pathogenesis of Crohn disease via IL-23/IFN-gamma axis. *J. Clin. Invest.* 2008. **118**: 2269–2280.

4 **Barish, G. D., Yu, R. T., Karunasiri, M., Ocampo, C. B., Dixon, J., Benner, C., Dent, A. L. et al.**, Bcl-6 and NF-kappaB cistromes mediate opposing regulation of the innate immune response. *Genes Dev.* 2010. **24**: 2760–2765.

5 **Ghisletti, S., Barozzi, I., Mietton, F., Polletti, S., De Santa, F., Venturini, E., Gregory, L. et al.**, Identification and characterization of enhancers controlling the inflammatory gene expression program in macrophages. *Immunity* 2010. **32**: 317–328.

6 **Ostuni, R., Piccolo, V., Barozzi, I., Polletti, S., Termanini, A., Bonifacio, S., Curina, A. et al.**, Latent enhancers activated by stimulation in differentiated cells. *Cell* 2013. **152**: 157–171.

7 **Krause, P., Morris, V., Greenbaum, J. A., Park, Y., Bjoerheden, U., Mikulski, Z., Muffley, T. et al.**, IL-10-producing intestinal macrophages prevent excessive antibacterial innate immunity by limiting IL-23 synthesis. *Nat. Commun.* 2015. **6**: 7055.

8 **Shouval, D. S., Biswas, A., Goettel, J. A., McCann, K., Conaway, E., Redhu, N. S., Mascanfroni, I. D. et al.**, Interleukin-10 receptor signaling in innate immune cells regulates mucosal immune tolerance and anti-inflammatory macrophage function. *Immunity* 2014. **40**: 706–719.

9 **Sellon, R. K., Tonkonogy, S., Schultz, M., Dieleman, L. A., Grenther, W., Balish, E., Rennick, D. M. et al.**, Resident enteric bacteria are necessary for development of spontaneous colitis and immune system activation in interleukin-10-deficient mice. *Infect. Immun.* 1998. **66**: 5224–5231.

10 **Sheikh, S. Z., Hegazi, R. A., Kobayashi, T., Onyiah, J. C., Russo, S. M., Matsuoka, K., Sepulveda, A. R. et al.**, An anti-inflammatory role for carbon monoxide and heme oxygenase-1 in chronic Th2-mediated murine colitis. *J. Immunol.* 2011. **186**: 5506–5513.

11 **Sheikh, S. Z., Matsuoka, K., Kobayashi, T., Li, F., Rubinas, T. and Plevy, S. E.**, Cutting edge: IFN-gamma is a negative regulator of IL-23 in murine macrophages and experimental colitis. *J. Immunol.* 2010. **184**: 4069–4073.

12 **Onyiah, J. C., Sheikh, S. Z., Maharshak, N., Steinbach, E. C., Russo, S. M., Kobayashi, T., Mackey, L. C. et al.**, Carbon monoxide and heme oxygenase-1 prevent intestinal inflammation in mice by promoting bacterial clearance. *Gastroenterology* 2013. **144**: 789–798.

13 **Simon, J. M., Giresi, P. G., Davis, I. J. and Lieb, J. D.**, Using formaldehyde-assisted isolation of regulatory elements (FAIRE) to isolate active regulatory DNA. *Nat. Protoc.* 2012. **7**: 256–267.

14 **Kobayashi, T., Matsuoka, K., Sheikh, S. Z., Russo, S. M., Mishima, Y., Collins, C., deZoeten, E. F. et al.**, IL-10 regulates Il12b expression via histone deacetylation: implications for intestinal macrophage homeostasis. *J. Immunol.* 2012. **189**: 1792–1799.

15 **Heinz, S., Benner, C., Spann, N., Bertolino, E., Lin, Y. C., Laslo, P., Cheng, J. X. et al.**, Simple combinations of lineage-determining transcription factors prime cis-regulatory elements required for macrophage and B cell identities. *Mol. Cell* 2010. **38**: 576–589.

16 **McLean, C. Y., Bristor, D., Hiller, M., Clarke, S. L., Schaar, B. T., Lowe, C. B., Wenger, A. M. et al.**, GREAT improves functional interpretation of cis-regulatory regions. *Nat. Biotechnol.* 2010. **28**: 495–501.

17 **Manrique, S. Z., Correa, M. A., Hoelzinger, D. B., Dominguez, A. L., Mirza, N., Lin, H. H., Stein-Streilein, J. et al.**, Foxp3-positive macrophages display immunosuppressive properties and promote tumor growth. *J. Exp. Med.* 2011. **208**: 1485–1499.

18 **Pello, O. M., De Pizzol, M., Mirolo, M., Soucek, L., Zammataro, L., Amabile, A., Doni, A. et al.**, Role of c-MYC in alternative activation of human macrophages and tumor-associated macrophage biology. *Blood* 2012. **119**: 411–421.

19 **Lang, R., Patel, D., Morris, J. J., Rutschman, R. L. and Murray, P. J.**, Shaping gene expression in activated and resting primary macrophages by IL-10. *J. Immunol.* 2002. **169**: 2253–2263.

20 **Yang, S., Gao, L., Lu, F., Wang, B., Gao, F., Zhu, G., Cai, Z. et al.**, Transcription factor myocyte enhancer factor 2D regulates interleukin-10 production in microglia to protect neuronal cells from inflammation-induced death. *J. Neuroinflammation* 2015. **12**: 33.

21 **Laslo, P., Spooner, C. J., Warmflash, A., Lancki, D. W., Lee, H. J., Sciammas, R., Gantner, B. N. et al.**, Multilineage transcriptional priming and determination of alternate hematopoietic cell fates. *Cell* 2006. **126**: 755–766.

22 **Uno, J. K., Rao, K. N., Matsuoka, K., Sheikh, S. Z., Kobayashi, T., Li, F., Steinbach, E. C. et al.**, Altered macrophage function contributes to colitis in mice defective in the phosphoinositide-3 kinase subunit p110delta. *Gastroenterology* 2010. **139**: 1642–1653, 1653 e1641–1646.

23 **Kobayashi, T., Matsuoka, K., Sheikh, S. Z., Elloumi, H. Z., Kamada, N., Hisamatsu, T., Hansen, J. J. et al.**, NFIL3 is a regulator of IL-12 p40 in macrophages and mucosal immunity. *J. Immunol.* 2011. **186**: 4649–4655.

24 **Takada, Y., Hisamatsu, T., Kamada, N., Kitazume, M. T., Honda, H., Oshima, Y., Saito, R. et al.**, Monocyte chemoattractant protein-1 contributes to gut homeostasis and intestinal inflammation by composition of IL-10-producing regulatory macrophage subset. *J. Immunol.* 2010. **184**: 2671–2676.

25 **Camp, J. G., Frank, C. L., Lickwar, C. R., Guturu, H., Rube, T., Wenger, A. M., Chen, J. et al.**, Microbiota modulate transcription in the intestinal epithelium without remodeling the accessible chromatin landscape. *Genome Res.* 2014. **24**: 1504–1516.

26 **Jostins, L., Ripke, S., Weersma, R. K., Duerr, R. H., McGovern, D. P., Hui, K. Y., Lee, J. C. et al.**, Host-microbe interactions have shaped the genetic architecture of inflammatory bowel disease. *Nature* 2012. **491**: 119–124.

27 **Shibata, Y., Sheffield, N. C., Fedrigo, O., Babbitt, C. C., Wortham, M., Tewari, A. K., London, D. et al.**, Extensive evolutionary changes in regulatory element activity during human origins are associated with altered gene expression and positive selection. *PLoS Genet.* 2012. **8**: e1002789.

28 **Berg, D. J., Davidson, N., Kuhn, R., Muller, W., Menon, S., Holland, G., Thompson-Snipes, L. et al.**, Enterocolitis and colon cancer in interleukin-10-deficient mice are associated with aberrant cytokine production and CD4(+) TH1-like responses. *J. Clin. Invest.* 1996. **98**: 1010–1020.

29 **Schreiber, S., Fedorak, R. N., Nielsen, O. H., Wild, G., Williams, C. N., Nikolaus, S., Jacyna, M. et al.**, Safety and efficacy of recombinant human interleukin 10 in chronic active Crohn's disease. Crohn's Disease IL-10 Cooperative Study Group. *Gastroenterology* 2000. **119**: 1461–1472.

30 **Glocker, E. O., Kotlarz, D., Boztug, K., Gertz, E. M., Schaffer, A. A., Noyan, F., Perro, M. et al.**, Inflammatory bowel disease and mutations affecting the interleukin-10 receptor. *N. Engl. J. Med.* 2009. **361**: 2033–2045.

31 **Dixon, J. R., Jung, I., Selvaraj, S., Shen, Y., Antosiewicz-Bourget, J. E., Lee, A. Y., Ye, Z. et al.**, Chromatin architecture reorganization during stem cell differentiation. *Nature* 2015. **518**: 331–336.

32 **McKay, D. J. and Lieb, J. D.**, A common set of DNA regulatory elements shapes Drosophila appendages. *Dev. Cell* 2013. **27**: 306–318.

33 **Paige, S. L., Thomas, S., Stoick-Cooper, C. L., Wang, H., Maves, L., Sandstrom, R., Pabon, L. et al.**, A temporal chromatin signature in human embryonic stem cells identifies regulators of cardiac development. *Cell* 2012. **151**: 221–232.

34 **Thomas, S.**, **Li, X. Y.**, **Sabo, P. J.**, **Sandstrom, R.**, **Thurman, R. E.**, **Canfield, T. K.**, **Giste, E. et al.**, Dynamic reprogramming of chromatin accessibility during Drosophila embryo development. *Genome Biol.* 2011. **12**: R43.

35 **Lavin, Y.**, **Winter, D.**, **Blecher-Gonen, R.**, **David, E.**, **Keren-Shaul, H.**, **Merad, M.**, **Jung, S. et al.**, Tissue-resident macrophage enhancer landscapes are shaped by the local microenvironment. *Cell* 2014. **159**: 1312–1326.

36 **Gomez Perdiguero, E.**, **Klapproth, K.**, **Schulz, C.**, **Busch, K.**, **Azzoni, E.**, **Crozet, L.**, **Garner, H. et al.**, Tissue-resident macrophages originate from yolk-sac-derived erythro-myeloid progenitors. *Nature* 2015. **518**: 547–551.

37 **Yanai, H. and Hanauer, S. B.**, Assessing response and loss of response to biological therapies in IBD. *Am. J. Gastroenterol.* 2011. **106**: 685–698.

38 **Herfarth, H. and Scholmerich, J.**, IL-10 therapy in Crohn's disease: at the crossroads. Treatment of Crohn's disease with the anti-inflammatory cytokine interleukin 10. *Gut* 2002. **50**: 146–147.

39 **Steinbach, E. C. and Plevy, S. E.**, The role of macrophages and dendritic cells in the initiation of inflammation in IBD. *Inflamm. Bowel Dis.* 2014. **20**: 166–175.

40 **Kobayashi, T.**, **Steinbach, E. C.**, **Russo, S. M.**, **Matsuoka, K.**, **Nochi, T.**, **Maharshak, N.**, **Borst, L. B. et al.**, NFIL3-deficient mice develop microbiota-dependent, IL-12/23-driven spontaneous colitis. *J. Immunol.* 2014. **192**: 1918–1927.

41 **Steinbach, E. C.**, **Gipson, G. R. and Sheikh, S. Z.**, Induction of murine intestinal inflammation by adoptive transfer of effector $CD4^+$ CD45RB high T cells into immunodeficient mice. *J Vis Exp* 2015. **98**: e52533.

42 **Carroll, T. S.**, **Liang, Z.**, **Salama, R.**, **Stark, R. and de Santiago, I.**, Impact of artifact removal on ChIP quality metrics in ChIP-seq and ChIP-exo data. *Front Genet.* 2014. **5**: 75.

43 **Bernstein, B. E.**, **Birney, E.**, **Dunham, I.**, **Green, E. D.**, **Gunter, C. and Snyder, M.**, An integrated encyclopedia of DNA elements in the human genome. *Nature* 2012. **489**: 57–74.

44 **Lassmann, T.**, **Hayashizaki, Y. and Daub, C. O.**, TagDust-a program to eliminate artifacts from next generation sequencing data. *Bioinformatics* 2009. **25**: 2839–2840.

45 **Wu, T. D. and Nacu, S.**, Fast and SNP-tolerant detection of complex variants and splicing in short reads. *Bioinformatics* 2010. **26**: 873–881.

46 **Boyle, A. P.**, **Guinney, J.**, **Crawford, G. E. and Furey, T. S.**, F-Seq: a feature density estimator for high-throughput sequence tags. *Bioinformatics* 2008. **24**: 2537–2538.

47 **Quinlan, A. R. and Hall, I. M.**, BEDTools: a flexible suite of utilities for comparing genomic features. *Bioinformatics* 2010. **26**: 841–842.

48 **Chen, K.**, **Xi, Y.**, **Pan, X.**, **Li, Z.**, **Kaestner, K.**, **Tyler, J.**, **Dent, S. et al.**, DANPOS: dynamic analysis of nucleosome position and occupancy by sequencing. *Genome Res.* 2013. **23**: 341–351.

49 **Mortazavi, A.**, **Williams, B. A.**, **McCue, K.**, **Schaeffer, L. and Wold, B.**, Mapping and quantifying mammalian transcriptomes by RNA-Seq. *Nat. Methods* 2008. **5**: 621–628.

50 **Anders, S. and Huber, W.**, Differential expression analysis for sequence count data. *Genome Biol.* 2010. **11**: R106.

51 **Campbell, P. J.**, **Stephens, P. J.**, **Pleasance, E. D.**, **O'Meara, S.**, **Li, H.**, **Santarius, T.**, **Stebbings, L. A. et al.**, Bowtie: an ultrafast memory-efficient short read aligner identification of somatically acquired rearrangements in cancer using genome-wide massively parallel paired-end sequencing. *Nat. Genet.* 2008. **40**: 722–729.

52 **Liu, E. Y.**, **Li, M.**, **Wang, W. and Li, Y.**, MaCH-admix: genotype imputation for admixed populations. *Genet. Epidemiol.* 2013. **37**: 25–37.

Abbreviations: **BMMs**: bone marrow derived macrophages · **CD**: Crohn's disease · **CR**: conventionally raised · **FAIRE**: Formaldehyde-Assisted Isolation of Regulatory Elements · **GF**: germ-free · ***Il10*$^{-/-}$**: IL-10-deficient · **IL10VARs**: IL-10 variable accessible regions · **IMs**: intestinal macrophages

Full correspondence: Dr. Shehzad Z. Sheikh, Department of Medicine, University of North Carolina at Chapel Hill, 7340B Medical Biomolecular Research Building, Chapel Hill, NC 27517, USA
e-mail: sheisx@med.unc.edu

Additional correspondence: Dr. Terrence S. Furey, Department of Genetics, University of North Carolina at Chapel Hill, 5022 Genetic Medicine Building, Chapel Hill, NC 27517, USA
e-mail: tsfurey@email.unc.edu

Received: 4/12/2015
Revised: 26/3/2016
Accepted: 4/5/2016
Accepted article online: 9/5/2016

